

SUB-BAND STAP FOR STRETCH PROCESSED SYSTEMS

Hasan Mir and Zachary Berkowitz

University of Washington

ABSTRACT

This paper considers adaptive jammer rejection algorithms applicable to wideband *stretch-processed* systems. Specifically, sub-banding algorithms in which the received data is first pre-processed into narrow frequency bins are studied. In conventional sub-band STAP, the received signal is divided into narrowband frequency bins, following which the interference is adaptively rejected in each bin. This usually requires that a different weight vector be computed for each sub-band. Alternatively, the received data can be pre-processed so that every sub-band is shifted to a common central sub-band. This enables computation of a single weight vector that can be applied to all of the shifted sub-bands. Simulation results are presented to assess the behavior and performance of these algorithms.

Index Terms— STAP, Adaptive beamforming, Stretch radar

1. INTRODUCTION

In order to create a high resolution target range profile, a digital array radar must employ a waveform with wide bandwidth. This in turn implies that the radar receiver must be capable of processing the wideband return signal.

Wideband system operation presents several challenges. Because of the wide waveform bandwidth, high-speed analog-to-digital converters (ADCs) are required to sample the return signal. However, the dynamic range and speed of an ADC are competing requirements. The reduced dynamic range of a high speed ADC will thus limit the ability of the system to perform in high clutter environments such as littoral regions. Another challenge of wideband systems is the ability to operate in the presence of co-channel interference/jamming. The wide bandwidth return waveforms introduce dispersion across the array, and thus the adaptive signal processing methods must be modified to combat this effect.

In order to address the problems associated with high-speed ADCs, stretch processing [1] may be employed. In stretch processing, the transmit waveform is a conventional wideband linear frequency modulated (LFM) waveform. However, the received wideband LFM waveform is mixed with an LFM waveform having the same slope as that of the transmit signal. After bandpass filtering, a tone whose

frequency is proportional to the target range results. By selecting a band of frequencies (which thus corresponds to a range window) to digitize, rather than entire RF bandwidth, usage of a much lower-speed ADC is possible.

Even with stretch processing, dispersive effects due to the wide waveform bandwidth will be present. One popular method to contend with wideband processing is the sub-band approach [2], [3]. That is, the receive signal is divided into many sub-bands in frequency, each of which is approximately narrowband. Conventional narrowband processing can then be applied to each sub-band.

This paper is organized as follows: Section 2 formulates the sub-band algorithms for stretch processed systems and describes their application. Section 3 presents and discusses the simulation examples of the these algorithms.

2. DEVELOPMENT

2.1. Stretch Processing

Consider a transmitted waveform $s_{TX}(t)$ and a “local oscillator” waveform $s_{LO}(t)$, both of which are LFM waveforms with identical chirp rate k and finite duration T . These waveforms may be expressed as

$$\begin{aligned} s_{TX}(t) &= \cos \left[2\pi \left(\frac{k}{2}t^2 + f_{TX}^{(i)}t \right) \right] \\ s_{LO}(t) &= \cos \left[2\pi \left(\frac{k}{2}t^2 + f_{LO}^{(i)}t \right) \right] \end{aligned}$$

where $f_{TX}^{(i)}$ and $f_{LO}^{(i)}$ are the respective initial frequencies. The received signal from a target can be expressed as $s_{TX}(t - \tau)$ for some delay τ . Mixing $s_{TX}(t - \tau)$ with the “local oscillator” waveform $s_{LO}(t)$ and bandpass filtering results in a tone with frequency

$$k\tau + \left(f_{LO}^{(i)} - f_{TX}^{(i)} \right). \quad (1)$$

The above sequence of operations is known as stretch processing. It can be seen from (1) that stretch processing results in a tone whose frequency is proportional to the target range. The bandpass filter that follows the mixing with $s_{LO}(t)$ is centered at $f_{LO}^{(i)} - f_{TX}^{(i)}$. The selected width of this filter corresponds to the target range window that is selected based

upon the range of interest and ADC capabilities. Thus, stretch processing accommodates wideband waveforms without the need for high-speed ADCs by confining the target range of interest to a relatively narrow frequency band.

2.2. Formulation

Consider a signal with frequency f arriving at angle θ on an N -element uniform linear array with inter-element spacing d . The array response vector can be expressed as

$$\mathbf{v}(\theta, f) = [v_1(\theta, f) \quad \dots \quad v_N(\theta, f)]^T \quad (2)$$

where

$$v_n(\theta, f) = e^{-j\frac{2\pi d}{c}(n-1)f \sin \theta}, n = 1 \dots N \quad (3)$$

and c denotes the speed of light.

Following the development in [4], the k th Fourier series coefficient of (3) can be written as

$$\begin{aligned} c_k &= \frac{1}{2\pi} \int_{-\pi}^{+\pi} e^{-j\left[\frac{2\pi d}{c}(n-1)f \sin \theta - k\theta\right]} d\theta \\ &= J_k\left(\frac{2\pi d}{c}(n-1)f\right) \end{aligned} \quad (4)$$

where $J_k(\cdot)$ denotes the order k Bessel function of the first kind. Thus,

$$\begin{aligned} v_n(\theta, f) &= \sum_{k=-\infty}^{+\infty} J_k\left(\frac{2\pi d}{c}(n-1)f\right) e^{-jk\theta} \\ &= \sum_{k=0}^{+\infty} J_k\left(\frac{2\pi d}{c}(n-1)f\right) \rho_k(\theta) \end{aligned} \quad (5)$$

where

$$\rho_k(\theta) = \begin{cases} 1 & k = 0 \\ e^{-jk\theta} + (-1)^k e^{+jk\theta} & k \geq 1 \end{cases} \quad (6)$$

As such, the array response vector using a K term Fourier expansion can be expressed as

$$\mathbf{v}(\theta, f) \approx \mathbf{J}(f) \boldsymbol{\rho}(\theta) \quad (7)$$

where

$$\begin{aligned} [\mathbf{J}(f)]_{nk} &= J_{k-1}\left(\frac{2\pi d}{c}(n-1)f\right) \\ [\boldsymbol{\rho}(\theta)]_k &= \rho_k(\theta) \end{aligned} \quad (8)$$

for $n = 1 \dots N$ and $k = 1 \dots K$. This technique will be termed as angle-frequency decoupling (AFD).

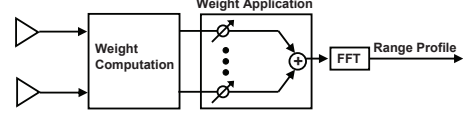


Fig. 1. Narrowband adaptive beamforming architecture.

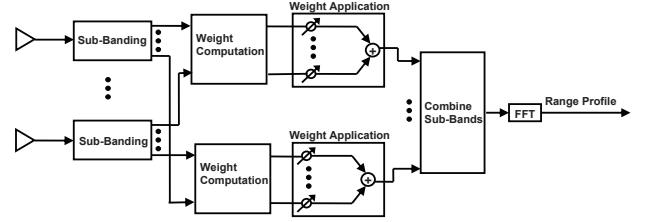


Fig. 2. Conventional sub-band STAP architecture.

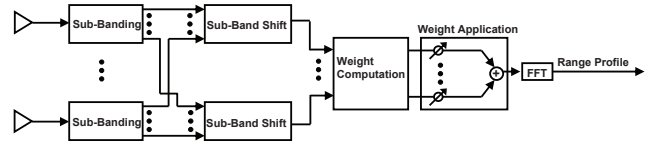


Fig. 3. AFD sub-band STAP architecture.

2.3. Adaptive Architectures

Various adaptive architectures are depicted in Figures 1-3.

Figure 1 shows the ABF architecture for narrowband signals. I/Q samples from each channel are used to form an adaptive weight vector (computed using e.g. the SMI method [5]) which is then applied to the data in order to reject interference. Note that because of the usage of stretch processing, an FFT is applied at the beamformer output to obtain the target range profile.

As previously discussed, the frequency dependence of the array response vector will manifest itself in the form of dispersive effects at wide bandwidths. This will lead to a degradation in the performance of the architecture in Figure 1, since adaptivity is present only in the spatial dimension. The addition of adaptivity in the temporal dimension as well results in a space-time adaptive processor (STAP) that can mitigate dispersive effects. In the sub-band STAP architecture shown in Figure 2, the I/Q data from each channel is first divided to into multiple narrow sub-bands. The sub-bands corresponding to the same frequency bin are grouped so that narrowband ABF may be applied to each bin.

Figure 3 shows the sub-band STAP architecture modified to use AFD. It can be seen from Figures 1-3 that the AFD sub-band STAP architecture is essentially a hybrid of the narrowband ABF and conventional sub-band STAP architecture; the I/Q data from all channels is shifted to a common sub-band, following which a single weight vector is computed.

One important advantage of stretch processing is that the sub-banding procedure is essentially free from a computational standpoint. In a conventional matched filter system, a filter bank would be necessary to divide the received data into sub-bands. With stretch processing, a natural time-frequency mapping exists, since time cells correspond to frequency bins. Thus, sub-banded data can be generated by simply grouping time-domain samples according to the desired sub-band width.

2.4. Application

Consider a wide bandwidth that is subdivided into M narrowband bins. To map an array response at frequency f_m , $m = 1 \dots M$ to a center frequency f_0 , a transformation matrix \mathbf{T}_m can be obtained as the solution to the least-squares optimization problem

$$\arg \min_{\mathbf{T}_m} \|\mathbf{T}_m \mathbf{J}(f_m) - \mathbf{J}(f_0)\|_2^2 \quad (9)$$

The solution is given by

$$\mathbf{T}_m = \mathbf{J}(f_0) \mathbf{J}^\#(f_m) \quad (10)$$

where $\#$ denotes the Moore-Penrose pseudo-inverse. It should be noted, however, that unless $\mathbf{T}_m \mathbf{T}_m^H = \mathbf{I}$, that is, \mathbf{T}_m is a unitary matrix, the noise statistics will change and result in noise inflation. In order to keep the noise uncorrelated, the optimization problem in (9) can be modified to include the constraint that \mathbf{T}_m be a unitary matrix. This problem is known as the *Orthonormal Procrustes Problem*, and the solution is given by

$$\mathbf{T}_m = \mathbf{V}_m \mathbf{U}_m^H \quad (11)$$

where \mathbf{V}_m and \mathbf{U}_m are matrices of the right and left singular vectors of the matrix

$$\mathbf{J}(f_m) \mathbf{J}^H(f_0) = \mathbf{U}_m \mathbf{\Sigma}_m \mathbf{V}_m^H$$

In summary, the AFD algorithm proceeds as follows:

1. Sub-band the sampled data $\mathbf{x}(t)$ into M frequency sub-bands, each of which is approximately narrowband, resulting is the sub-banded data $\mathbf{x}_m(t)$, $m = 1 \dots M$.
2. Form the transformation matrix \mathbf{T}_m , $m = 1 \dots M$, for each sub-band m .
3. Compute the adaptive weight vector using the shifted sub-banded data vectors $\mathbf{T}_m \mathbf{x}_m(t)$, $m = 1 \dots M$.
4. Apply the adaptive weight vector to each shifted sub-band.

3. SIMULATION RESULTS AND DISCUSSION

A simulation is performed to assess the performance of the architectures discussed in Section 2.3. For all simulations, a 20 element array with half-wavelength spacing at 480 MHz is assumed. Stretch processing is performed using a 100 MHz bandwidth LFM waveform that spans an RF range of 430 MHz to 530 MHz. The IF filter bandwidth is set at 10 MHz, and a 0 dB SNR target incident from 50° (0° is broadside) is assumed.

In Figures 4-7, a 20 dB JNR jammer is assumed incident from 45° . Figures 4-6 show the narrowband ABF, conventional sub-band STAP, and AFD sub-band STAP beampattern. The frequency dispersion in the narrowband adaptive beamforming beampattern in Figure 4 is evident. Figures 5 and 6 both show that the usage of STAP enables maintaining a null in the jammer direction while keeping the mainbeam on the target for the entire RF bandwidth. Figure 7 shows the resulting target range profile using the different processing architectures. Due to the dispersive null, narrowband ABF results in very weak peak, while both conventional and AFD sub-band STAP result in a pronounced detection.

Figure 8 shows the SINR as the jammer angle is varied. Again, it is apparent that narrowband ABF suffers from dispersive effects, while conventional and AFD sub-band STAP result in much higher SINR levels. An alternate view of this is presented in Figure 9, wherein the level of the target peak for conventional and AFD sub-band STAP has been normalized to 0 dB. It is apparent that AFD sub-band STAP has much improved sidelobe levels compared to conventional sub-band STAP. As noted in [2], conventional sub-band STAP suffers from elevated range sidelobes due to the fluctuation in the response of the adaptive weight vector from one sub-band to another. This phenomena is mitigated by the fact that AFD sub-band STAP computes only a single adaptive weight vector.

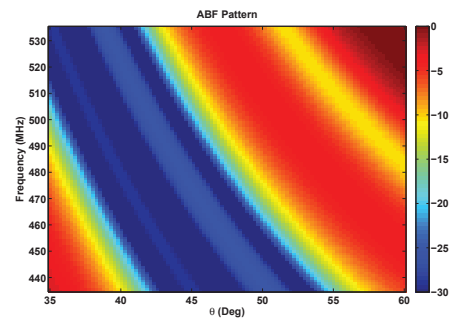


Fig. 4. Narrowband adaptive beamforming beampattern.

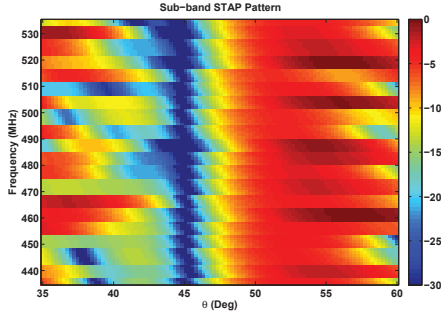


Fig. 5. Conventional sub-band STAP beampattern.

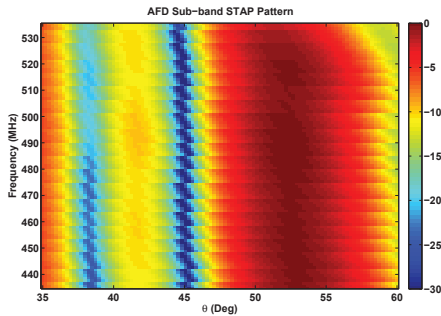


Fig. 6. AFD sub-band STAP beampattern.

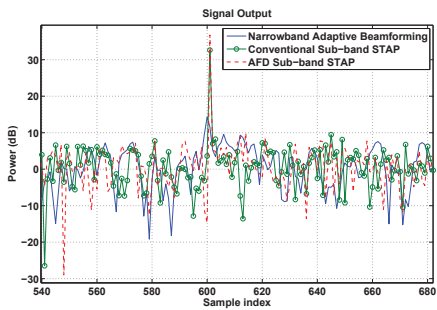


Fig. 7. Target range profile.

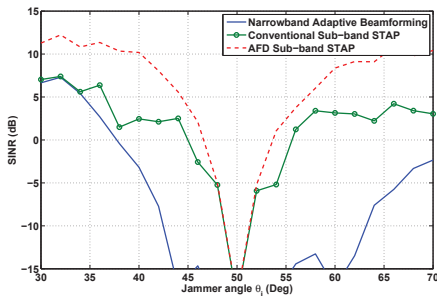


Fig. 8. SINR as a function of jammer angle.

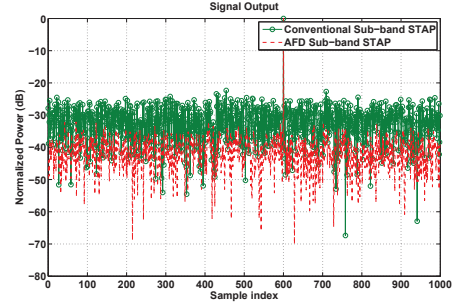


Fig. 9. Comparison of range sidelobe levels.

4. CONCLUSION

Stretch processed systems offer a means of achieving wide system bandwidth without the need for high-speed ADCs. Nonetheless, dispersive effects due to bandwidth still persist, and necessitate the application of STAP in order to maintain a jammer null and target mainbeam over wide bandwidths. The conventional sub-band STAP architecture partitions the data in narrow sub-bands and computes an adaptive weight vector for each sub-band. AFD sub-band STAP takes advantage of the decoupling of the angle and frequency components of the array response vector that is possible using a Bessel function series expansion. This decoupling allows the sub-bands to be focused to a common center sub-band, following which only a single adaptive weight vector need be computed. Simulation results verify the efficacy of AFD sub-band STAP and show that it can offer improved performance over conventional sub-band STAP.

5. REFERENCES

- [1] W. J. Caputi, "Stretch: A time-transformation technique," *IEEE Trans. Aerosp. Electron. Syst.*, vol. AES-7, no. 2, pp. 269 - 278, Mar. 1971.
- [2] D.J. Rabideau and P. Parker, "Wideband adaptive beamforming to control time sidelobes and null depth," *Proceedings of SPIE*, vol. 5077, pp. 187 - 199, Apr. 2003.
- [3] J. A. Torres et al, "Efficient wideband jammer nulling when using stretch processing," *IEEE Trans. Aerosp. Electron. Syst.*, vol. AES-36, no. 4, pp. 1167 - 1178, Oct. 2000.
- [4] S. Pillai, K. Li, and J. Guerci "Efficient Wideband Processing Without Subbanding," *2008 IEEE Radar Conference*, pp. 1199-1203, May 2008.
- [5] H. Van Trees, *Optimum Array Processing (Detection, Estimation, and Modulation Theory, Part IV)*, Wiley-Interscience, 2002.